TDP-43 mutant transgenic mice develop features of ALS and frontotemporal lobar degeneration

Iga Wegorzewska[a], Shaughn Bell[a], Nigel J. Cairns[a,b], Timothy M. Miller[a,b], and Robert H. Baloh[a,b,1]

[a]Department of Neurology and [b]Hope Center for Neurological Diseases, Washington University School of Medicine, 660 South Euclid Avenue, St. Louis, MO 63110

Edited by L. L. Iversen, University of Oxford, Oxford, United Kingdom, and approved September 4, 2009 (received for review August 3, 2009)

Frontotemporal lobar degeneration (FTLD) and amyotrophic lateral sclerosis (ALS) are neurodegenerative diseases that show considerable clinical and pathologic overlap, with no effective treatments available. Mutations in the RNA binding protein TDP-43 were recently identified in patients with familial amyotrophic lateral sclerosis (ALS), and TDP-43 aggregates are found in both ALS and FTLD-U (FTLD with ubiquitin aggregates), suggesting a common underlying mechanism. We report that mice expressing a mutant form of human TDP-43 develop a progressive and fatal neurodegenerative disease reminiscent of both ALS and FTLD-U. Despite universal transgene expression throughout the nervous system, pathologic aggregates of ubiquitinated proteins accumulate only in specific neuronal populations, including layer 5 pyramidal neurons in frontal cortex, as well as spinal motor neurons, recapitulating the phenomenon of selective vulnerability seen in patients with FTLD-U and ALS. Surprisingly, cytoplasmic TDP-43 aggregates are not present, and hence are not required for TDP-43-induced neurodegeneration. These results indicate that the cellular and molecular substrates for selective vulnerability in FTLD-U and ALS are shared between mice and humans, and suggest that altered DNA/RNA-binding protein function, rather than toxic aggregation, is central to TDP-43-related neurodegeneration.

dementia | motor neuron disease | neurodegeneration | protein aggregation

FTLD is a relatively common cause of dementia among patients with onset before 65, typically manifesting with behavioral changes or language impairment due to degeneration of subpopulations of cortical neurons in the frontal, temporal and insular regions (1). By contrast, ALS presents with muscle weakness and spasticity due to degeneration of motor neurons in both layer 5 of cortex and in the spinal cord, resulting in death from respiratory failure in 3–5 years (2, 3). Interestingly, approximately 20% of patients with ALS also develop FTLD, and approximately 15% of FLTD patients also develop ALS (4, 5).

The discovery that TDP-43 is present in cytoplasmic aggregates in both ALS and FTLD-U provided evidence that the two disorders may share a common underlying mechanism (6). TDP-43 is an RNA/DNA binding protein, implicated in regulation of alternative splicing of messenger RNA, RNA stability, and transcriptional control (7). The concept that TDP-43 can play a direct role in neurodegeneration was strengthened by recent reports that dominantly inherited missense mutations in TDP-43 are found in patients with familial ALS (8–12). Mutations in TDP-43 associated with ALS cluster in the C-terminal glycine-rich region, which is involved in protein-protein interactions between TDP-43 and other heterogeneous nuclear ribonuclear proteins (hnRNPs) (13). Furthermore, C-terminal fragments of TDP-43 are observed selectively in ALS and FTLD-U tissues, suggesting that proteolytic cleavage of TDP-43 leads to protein aggregation or another toxic property (6). Therefore, several putative mechanisms of TDP-43 induced neurodegeneration are currently under investigation, including toxic protein aggregation, and/or disruption of normal TDP-43 RNA/DNA binding protein function. Here we report a mouse model of TDP-43 induced neurodegeneration which recapitulates key features of ALS and FTLD-U, including ubiquitin aggregate pathology with selective vulnerability of cortical projection neurons and spinal motor neurons, but without the presence of TDP-43 aggregates. Together with recent reports of mutations in another RNA binding protein (*FUS/TLS*) in familial ALS (14, 15), this supports that altered RNA-binding protein function (rather than toxic aggregation of TDP-43) likely plays a central and unexpected role in ALS pathogenesis.

Results

To investigate the mechanism by which TDP-43 mutations lead to neurodegeneration, we generated transgenic mice expressing a human TDP-43 construct containing the A315T mutation seen in familial ALS patients (8), under the control of the mouse prion protein (Prp) promoter (Fig. 1*A*). Prp-TDP43^{A315T} mice were born at normal Mendelian ratios, weighed the same as nontransgenic littermates and appeared normal up to 3 months of age. Spinal cord lysates from Prp-TDP43^{A315T} mice showed that the exogenous TDP43^{A315T} protein ran at a slightly higher molecular weight due to the presence of the amino-terminal Flag tag, and was present at levels approximately 3-fold higher than endogenous mouse TDP-43 (Fig. 1*B*). Analysis of tissue lysates using an anti-Flag antibody showed that the Prp-TDP43^{A315T} transgene was expressed highest in the brain and spinal cord, but was also expressed at lower levels in most other tissues, a typical pattern for the Prp promoter (16) (Fig. 1*C*). Immunohistochemistry using an anti-Flag antibody to selectively visualize the exogenous TDP43^{A315T} transgene product showed nuclear staining in both neurons and glia throughout the brain and spinal cord, similar to endogenous TDP-43 (Fig. 1 *D–G* and Fig. S1).

Although they initially appeared normal and weighed the same as their littermates, Prp-TDP43^{A315T} mice developed a gait abnormality by approximately 3–4 months of age (Movie S1). By approximately 4.5 months of age Prp-TDP43^{A315T} mice began losing weight and developed a characteristic "swimming" gait, where they were unable to hold their body off the ground, but could still use their limbs for propulsion to slide on their stomachs (Fig. 1*H* and Movie S2). During this end-stage they either died spontaneously, or were euthanized if they were unable to obtain food or water. Average survival was 154 ± 19 days (Fig. 1*I*).

Ubiquitinated aggregates are the defining feature of FTLD-U (17), and are a prominent finding in both the brain and spinal cord of ALS patients (18). Therefore we examined brains of late stage Prp-TDP43^{A315T} mice using ubiquitin immunohistochem-

Author contributions: I.W. and R.H.B. designed research; I.W., S.B., and R.H.B. performed research; N.J.C. and T.M.M. contributed new reagents/analytic tools; I.W. and R.H.B. analyzed data; and I.W. and R.H.B. wrote the paper.

The authors declare no conflict of interest.

This article is a PNAS Direct Submission.

Freely available online through the PNAS open access option.

[1]To whom correspondence should be addressed. E-mail: rbaloh@wustl.edu.

This article contains supporting information online at www.pnas.org/cgi/content/full/0908767106/DCSupplemental.

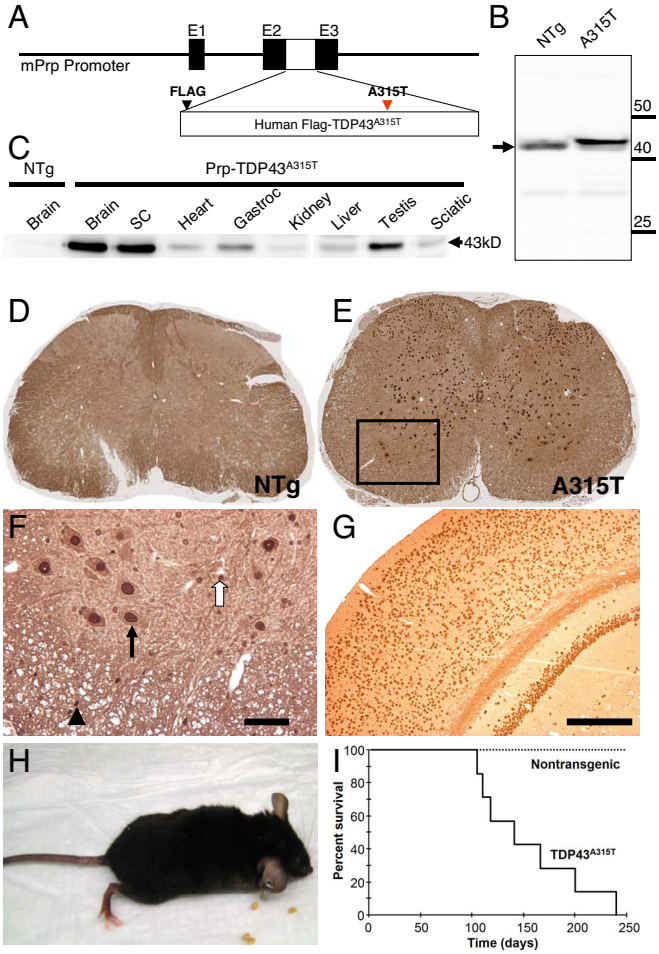

Fig. 1. Expression of a disease mutant form of TDP-43 throughout the nervous system in mice leads to progressive gait disturbance, and premature death. (*A*) Schematic diagram of the Prp-TDP43^{A315T} construct. A cDNA encoding a Flag-tagged human TDP-43 protein with the A315T point mutation seen in patients with familial ALS was placed into the mouse Prion protein promoter construct (mPrp). (*B*) Western blotting of brain lysates from nontransgenic (NTg) and Prp-TDP43^{A315T} mice (A315T) using an anti-TDP43 antibody showed a slight shift to a higher molecular weight due to the presence of the Flag tag, and approximately 3-fold higher levels compared to endogenous TDP-43 (arrow). (*C*) Western blotting of tissue lysates with anti-Flag antibody (specific for the human transgene) showed highest levels in brain, spinal cord, and testis, with lower levels in skeletal muscle (Gastroc–gastrocnemius), heart and other tissues. (*D–G*) Immunohistochemistry with anti-Flag antibody showed expression of the TDP43^{A315T} protein throughout the spinal cord (*E*–''A315T''), which was absent from nontransgenic animals (*D*–''NTg''). (*F*) Higher power image of area corresponding to the boxed region in *E*, showing that TDP43^{A315T} mutant protein was present in nuclei of large ventral horn motor neurons (arrow), as well as smaller nuclei in white matter tracts (arrowhead) and throughout the neuropil (open arrow) presumably corresponding to oligodendroglia and astrocytes. (Scale bar, 50 μm.) (*G*) Similar widespread expression was observed in the brain in neurons and non-neuronal cells, including all layers of cortex and hippocampus. (Scale bar, 200 μm.) (*H*) Photograph of end-stage Prp-TDP43^{A315T} mouse ($\approx$5 months old), unable to move its hindlimbs or right itself when placed on its back. (*I*) Survival curve of Prp-TDP43^{A315T} mice showed an average survival of 153 days. No Prp-TDP43^{A315T} mice have survived beyond 240 days.

istry. Remarkably, despite the universal expression of the Prp-TDP43^{A315T} transgene in all layers of cortex, we found cytoplasmic accumulation of ubiquitinated proteins selectively in neurons of cortical layer 5 (Fig. 2 *A* and *B*). Layer 5 cortical neurons with increased ubiquitin staining typically had the appearance of pyramidal cells (Fig. 2*C*), and were prominent in motor cortex, although they were also present in orbital, cingulate, sensory and other cortical regions (Table S1). Although the Prp-TDP43^{A315T} transgene was universally expressed in the nervous system including caudate/putamen, substantia nigra, thalamus and other structures, no ubiquitin aggregates were observed in these areas even in late stage Prp-TDP43^{A315T} mice. Increased cytoplasmic ubiquitin staining was either diffuse, punctate with multiple small aggregates, or in the form of large organized cytoplasmic aggregates (Fig. 2*D*). Glial fibrillary acidic protein staining was also selectively increased in cortical layer 5, suggesting that neuronal degeneration in this region leads to activation of local astrocytes and microglia (Fig. 2*J* and Fig. S2). Indeed, a decreased number of neurons in layer 5 were seen both on Nissl stain, and SMI32 immunostaining which labels nonphosphorylated neurofilament and is selectively enriched in layer 5 pyramidal projection neurons (19) (Fig. S3). Notably, aggregates of the Tau protein or α-synuclein were not present, another defining characteristic of FTLD-U brain pathology (17). Therefore Prp-TDP43^{A315T} mice develop neuronal cytoplasmic ubiquitinated inclusions with striking similarities to those seen in human FTLD-U. Importantly, despite the widespread expression of the Prp-TDP43^{A315T} transgene, there is remarkably selective involvement of certain neuronal subpopulations, including cortical upper motor neurons.

Cytoplasmic aggregates of TDP-43, together with loss of normal nuclear TDP-43 staining, are a common feature in vulnerable neurons in both FTLD-U and ALS (6, 20). However, immunohistochemical analysis of Prp-TDP43^{A315T} mouse brains using multiple different antibodies to TDP-43 did not show obvious cytoplasmic aggregates or inclusions, despite the striking abnormalities seen with ubiquitin immunostaining shown above. Therefore we performed double immunofluorescence to label both ubiquitin aggregates and TDP-43. We found that loss of nuclear TDP-43 staining was occasionally seen in neurons with ubiquitin positive inclusions, similar to what has been reported in human FTLD-U and ALS (20) (Fig. 2 *E–G*). By contrast, loss of nuclear TDP-43 was never seen in cortical layer 5 neurons of nontransgenic littermate controls. Surprisingly, ubiquitinated cytoplasmic inclusions were not positive for TDP-43 (Fig. 2 *H* and *I*). Although it is difficult to exclude the possibility that rare aggregates may contain TDP-43, we examined >100 ubiquitinated cytoplasmic inclusions in multiple Prp-TDP43^{A315T} mice, using antibodies directed toward either the amino- or carboxy-terminus of TDP-43, and did not find any inclusions which were positive for TDP-43. This finding indicates that the ubiquitin aggregate pathology and neurodegeneration found in selective brain regions of Prp-TDP43^{A315T} mice does not require the formation of large cytoplasmic TDP-43 aggregates.

Given that the TDP-43 A315T mutation was identified in families with ALS, we analyzed the motor system of Prp-TDP43^{A315T} mice. Amyotrophic lateral sclerosis is a clinicopathologic term coined by the famed neurologist Charcot to describe both muscle atrophy due to degeneration of spinal motor neurons (amyotrophy), together with axonal degeneration and sclerosis of the lateral columns of the spinal cord, which contain the corticospinal tract in humans (21). Examination of the lower thoracic spinal cord revealed fewer axons with numerous degenerating axons present in both the dorsal corticospinal tract and lateral columns (Fig. 3 *A–E*), indicating there is degeneration of descending motor axons in Prp-TDP43^{A315T} mice. To investigate abnormalities in spinal lower motor neurons, we performed ubiquitin immunohistochemistry on spinal cord sections. Similar to the findings in cortical layer 5 in brain, ubiquitin pathology was found to preferentially involve large neurons of the ventral horn as well as scattered interneurons (Fig. 3 *F* and *G*), despite expression of the Prp-TDP43^{A315T} transgene in all neurons and glia in the spinal cord (Fig. 1*E*). Spinal motor neurons with ubiquitin aggregates also at times

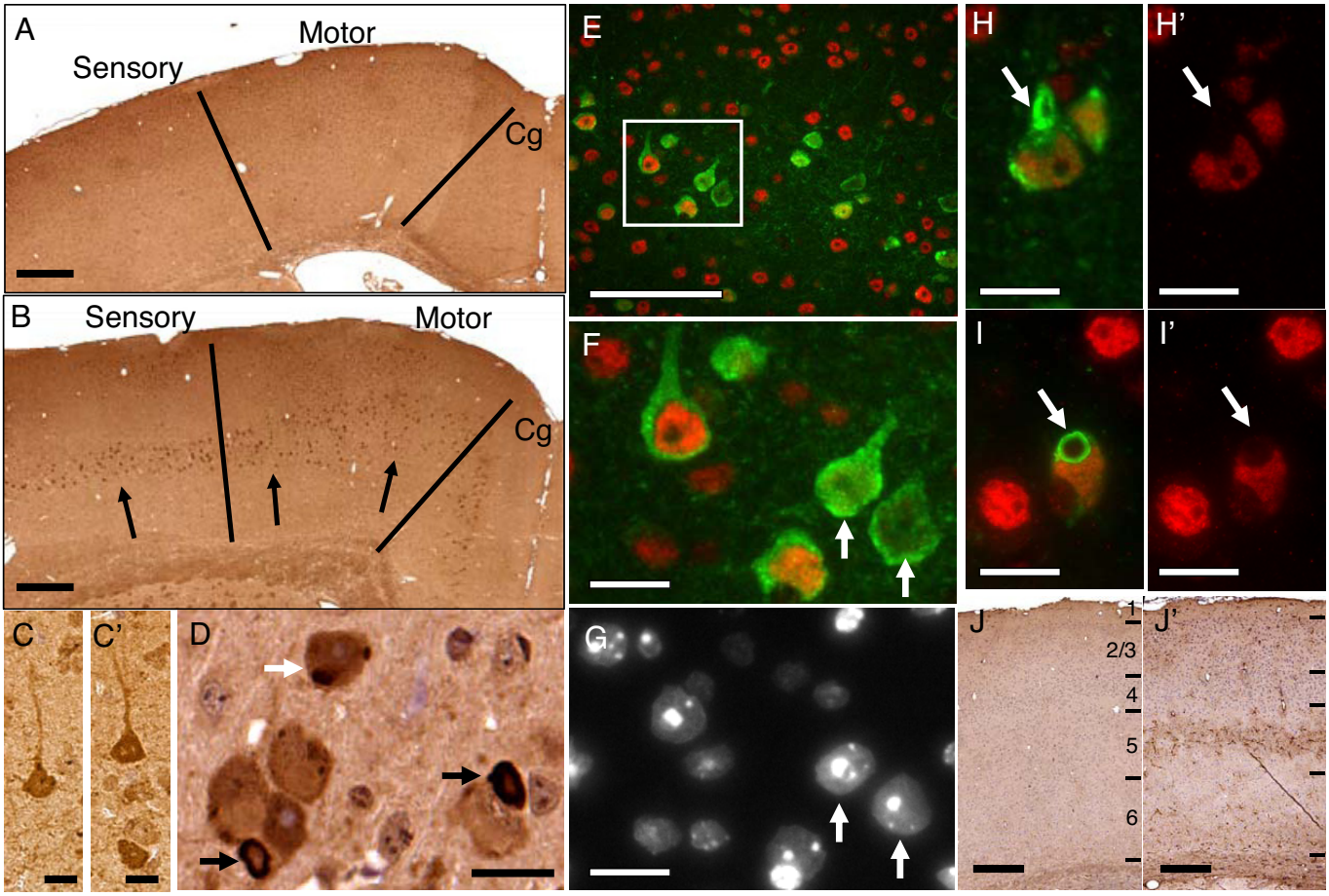

Fig. 2. Selective brain pathology in Prp-TDP43^{A315T} mice reminiscent of FTLD-U. (*A–D*) Ubiquitin immunohistochemical analysis of a non-transgenic (*A*) and late stage (4.5-month-old) Prp-TDP43^{A315T} brain (*B*) showing ubiquitin pathology (arrows) selectively in a population of layer 5 neurons in motor, sensory and cingulate (Cg) cortex, despite universal expression of the transgene in all cortical layers and throughout the brain. (Scale bars, 300 μm.) (*C* and *C'*) Ubiquitin accumulation was predominantly in pyramidal neurons, as either discrete cytoplasmic aggregates (*C*) or diffusely increased cytoplasmic staining (*C'*). (Scale bars, 10 μm.) (*D*) Some neurons contained large organized ubiquitin-positive cytoplasmic inclusions (black arrows), whereas others contained multiple smaller aggregates (white arrow). (Scale bar, 10 μm.) (*E–I*) Double immunostaining with antibodies to the C terminus of TDP-43 (red) and ubiquitin (green). (*E*) Some neurons with ubiquitin pathology showed loss of nuclear TDP-43 staining. (Scale bar, 50 μm.) (*F*) Higher power image of boxed region from (*E*), showing neurons with diminished nuclear TDP-43 staining (arrows). (*G*) DAPI staining of same field as (*F*) showing that nuclear structure is intact in neurons that have lost TDP-43 staining (white arrows indicate the same cells in *F* and *G*), indicating loss of TDP-43 occurs before neuron degeneration. (*H* and *I*) Overlay image of double immunofluorescence for ubiquitin (green) and TDP-43 (red) showing typical large cytoplasmic ubiquitinated aggregates (white arrows). (*H'* and *I'*) The same images showing only TDP-43 staining. Notably, ubiquitin-positive aggregates did not contain TDP-43. (Scale bars for *F* through *I*, 10 μm.) (*J* and *J'*) GFAP immunostaining was also selectively increased in cortical layer 5 of Prp-TDP43^{A315T} mice (*J'*) as compared to controls (*J*), indicating a reactive astrocytosis in the region of degenerating neurons with ubiquitin pathology. (Scale bars, 200 μm.)

displayed loss of nuclear TDP-43 staining, but again no cytoplasmic aggregates of TDP-43 were observed (Fig. S4). In addition to ubiquitin aggregate pathology, there was an approximately 20% loss of spinal motor neurons in end-stage Prp-TDP43^{A315T} mice (Fig. 3*H*). Examination of the femoral motor and sensory nerves revealed a loss of axons with features of ongoing axonal degeneration in the motor branch (Fig. S5). Muscle histology from end-stage Prp-TDP43^{A315T} mice showed scattered and grouped atrophic muscle fibers, a characteristic finding of denervation in muscle from patients with ALS (22) (Fig. 3 *I* and *J*). Furthermore, electromyography performed on end-stage Prp-TDP43^{A315T} mice showed numerous fibrillation potentials indicative of loss of muscle fiber innervation and fasciculations, which are spontaneous firing of motor units commonly seen in human motor neuron diseases (Fig. 3 *K* and *L*). Of note, muscle histology and electromyography of presymptomatic (2 months) and early symptomatic Prp-TDP43^{A315T} mice (≈3 months) were normal, whereas axonal degeneration in the spinal cord was already evident. Therefore the early gait abnormality in Prp-TDP43^{A315T} mice may be due to disruption of descending or ascending pathways in the spinal cord, but is not due to loss of muscle innervation. Furthermore, the approximate 20% loss of motor neurons at end stage indicates that either upper motor neuron loss or lower motor neuron dysfunction are responsible for the severe weakness and death in these mice. These findings indicate that Prp-TDP43^{A315T} mice develop motor neuron disease, with involvement of both cortical and spinal motor neurons, reminiscent of human ALS.

TDP-43 is known to be cleaved into C-terminal fragments, a finding observed only in tissue from patients with FTLD-U and ALS, but not Alzheimer's disease or other controls (6, 23). Recent evidence suggests that these fragments may themselves be toxic, and disrupt normal TDP-43 mediated alternative mRNA splicing (24). Immunoblotting of brain or spinal cord lysates from Prp-TDP43^{A315T} mice using an antibody to the Flag epitope, located at the N terminus immediately after the start methionine, showed only a single band at 43 kDa (Fig. 4*A*). However, immunoblotting with polyclonal antibodies raised to

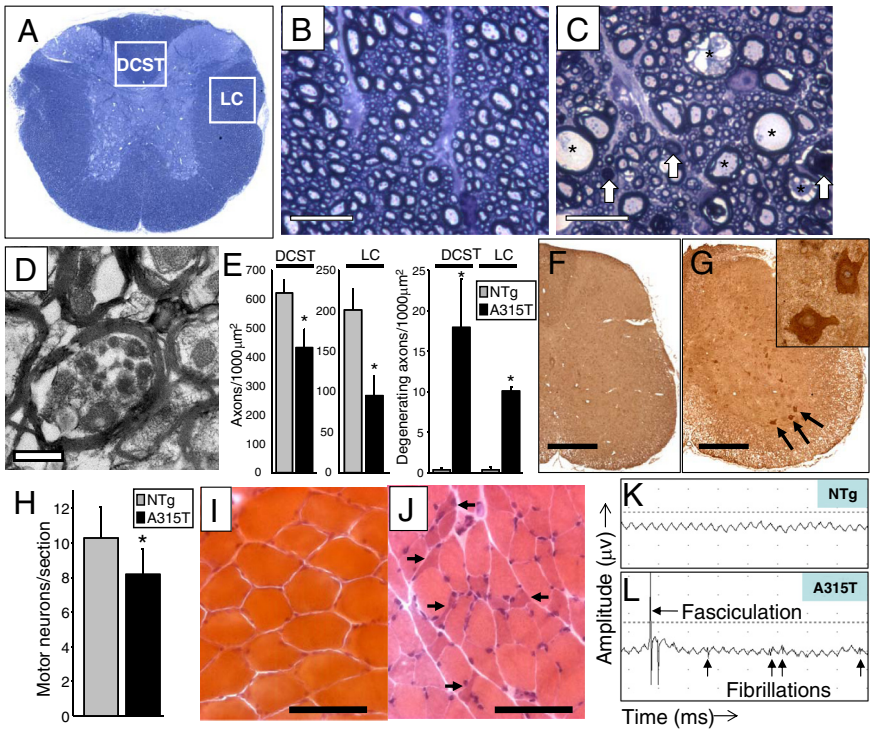

Fig. 3. Prp-TDP43^{A315T} mice develop motor neuron disease. (*A*) Toluidine blue stained section of lower thoracic spinal cord, indicating regions of descending motor pathways in the mouse, including the dorsal corticospinal tract (DCST) and lateral columns (LC). (*B* and *C*) Lateral columns from an end-stage nontransgenic Prp-TDP43^{A315T} mouse (*C*) showed both large dilated axons (asterisks) and degenerating axons (white arrows) in descending motor axons in Prp-TDP43^{A315T} mice that were not present in age-matched nontransgenic controls (*B*). (Scale bar, 10 μm.) (*D*) Electron micrograph of dorsal corticospinal tract axons from Prp-TDP43^{A315T} mouse, showing accumulations of dark axoplasmic material in a degenerating corticospinal tract axon. (Scale bar, 500 nm.) (*E*) Fewer axons were present in the DCST and LC of Prp-TDP43^{A315T} mice (A315T) as compared to nontransgenic controls (NTg), with more degenerating fibers seen in Prp-TDP43^{A315T} mice ($*$ = *t* test, $P < 0.05$). (*F* and *G*) Ubiquitin immunohistochemistry of spinal cord from a nontransgenic control (*F*) and a Prp-TDP43^{A315T} mouse (*G*), showing an increase in ubiquitin staining in lower motor neurons (black arrows, and inset), as well as scattered interneurons in Prp-TDP43^{A315T} mice. (Scale bars, 400 μm.) (*H*) Quantitation of motor neurons from the L3–L5 region showed an approximate 20% reduction in motor neurons in Prp-TDP43^{A315T} mice compared to nontransgenic controls ($*$ = *t* test, $P < 0.01$). Hematoxylin and eosin stain of muscle from a non-transgenic (*I*) and Prp-TDP43^{A315T} mouse (*J*), showing scattered and grouped muscle fiber atrophy, characteristic of motor axon degeneration. (Scale bars, 60 μm.) Electromyography from a 4-month-old Prp-TDP43^{A315T} mouse (*L*–A315T) showing fibrillations and fasciculations, common findings in ALS indicative of muscle fiber denervation and motor unit degeneration/regeneration. These findings were never present in nontransgenic (*K*–NTg) mice.

TDP-43 showed full length TDP-43, as well as additional C-terminal fragments at approximately 35 kDa and 25 kDa (Fig. 4 *B* and *C*) not present in nontransgenic littermate controls. These are identical in size to the fragments observed in nervous tissue from FTLD-U and ALS patients, but not in patients with other neurodegenerative diseases (6, 23). Previous reports have observed C-terminal TDP-43 fragments in both the detergent soluble and insoluble fractions, typically with enrichment in the insoluble phase (23). In contrast, we found that TDP-43 C-terminal fragments are predominantly in the detergent soluble fraction, with little or none seen in the detergent insoluble phase (Fig. 4*B*), consistent with the fact that we do not observe TDP-43 aggregates on histology. To further define when the C-terminal fragments appear in relationship to gait abnormalities and development of ubiquitin aggregate pathology, we examined brain and spinal cord lysates from Prp-TDP43^{A315T} mice of multiple ages. Interestingly we found that the C-terminal fragments of TDP-43 appeared between 1–2 months of age, before the onset of the gait disorder (≈3 months), and increased slightly over the next several months (Fig. 4*C*). As shown in Fig. 2 loss of nuclear TDP-43 staining was seen in neurons with ubiquitinated inclusions, suggesting that C-terminal fragmentation may simply coincide with degradation and loss of nuclear TDP-43. However, at 1 and 2 months of age, when C-terminal fragments are easily visualized, ubiquitin aggregates are rare and neurons with loss of nuclear TDP-43 were not seen (Fig. S6). These data indicate that Prp-TDP43^{A315T} mice develop C-terminal fragmentation of TDP-43 at an early stage before the onset of gait abnormalities or significant brain pathology, and are consistent with the idea that C-terminal fragments could play a direct role in TDP-43 associated neurodegeneration (24, 25).

Discussion

Selective vulnerability of certain neuronal populations is one of the fundamental features of neurodegenerative disease. It defines the core features of the clinical syndrome (i.e., weakness due to motor neuron loss in ALS, or slowness of movement and rigidity due to loss of substantia nigra neurons in Parkinson's disease), however the molecular and cellular basis of selective vulnerability in neurodegenerative diseases remains poorly understood. The fact that Prp-TDP43^{A315T} mice develop degeneration of specific neuronal populations suggests that the cellular and molecular substrates for selective vulnerability in FTLD-U and ALS are shared between mice and humans. Therefore the use of Prp-TDP43^{A315T} mice to explore the mechanisms of FTLD-U and ALS pathogenesis, as well as for studying therapeutic interventions for these diseases, holds great promise.

Despite additional attempts, we were unable to generate additional transgenic lines expressing the wild-type TDP-43 and TDP43^{A315T} mutant cDNAs under control of the Prion promoter for comparison to line reported here. We interpret this as evidence for selective pressure against expression of TDP-43

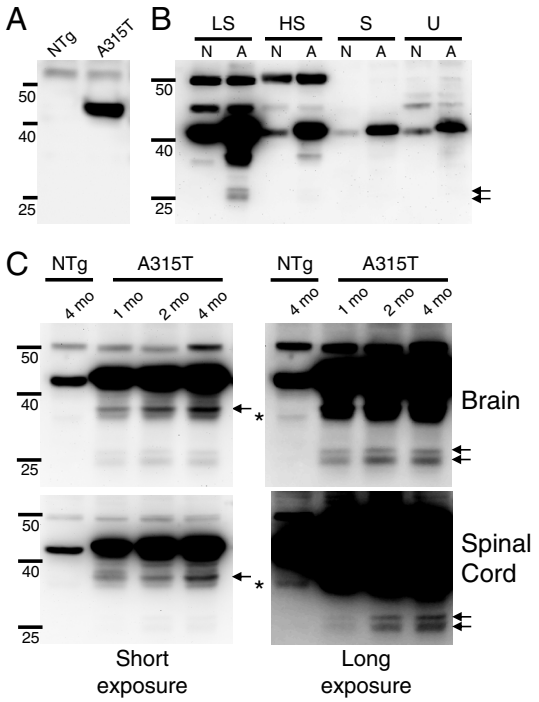

Fig. 4. Prp-TDP43^{A315T} mice show C-terminal fragmentation of TDP-43 in the presymptomatic phase. (*A*) Immunoblot of spinal cord lysates from 2-month-old non-transgenic (NTg) and Prp-TDP43^{A315T} (A315T) mice using an antibody to the Flag epitope located at the N terminus of the transgene. Only a single band is observed at approximately 43 kDa. (*B*) TDP43 immunoblot of serial fractions of brain from a non-transgenic (N) and Prp-TDP43^{A315T} mouse (*A*). Fractions shown are low salt (LS), high salt with Triton-X100 (HS), sarkosyl buffer (S), and urea buffer (U). Both full-length and C-terminal fragments (arrows) are predominant in the LS soluble fraction. (*C*) Immunoblots of the detergent soluble phase of brain and spinal cord lysates from either presymptomatic (1 month, 2 months) or late symptomatic (4 months) Prp-TDP43^{A315T} mice, using a polyclonal anti-TDP43 antibody raised to amino acids 1–260 (of 414). On shorter exposures (left panels) multiple smaller fragments of TDP43 at approximately 35 kDa were seen (arrow), which were already present by 1 month of age in both brain and spinal cord. Longer exposures (right panel) also revealed two bands at approximately 24 kDa and 26 kDa (arrows) which were present before symptom onset, and appeared to increase during the disease course. A faint single band at approximately 34 kDa is seen in the age-matched nontransgenic control tissue on long exposure, which likely represents a known splice form of endogenous mouse TDP-43 (asterisk). However the 35 kDa, 26 kDa, and 24 kDa C-terminal fragments were never seen in non-transgenic littermate controls.

above endogenous levels during early development, possibly related to its role in suppressing cell cycle observed in an immortalized epithelial cell line in vitro (26). Although we cannot determine from our analysis whether a comparable phenotype would be observed with a similar level of overexpression of the wild-type TDP-43 cDNA, the selective toxicity to layer 5 cortical neurons and motor neurons argues strongly that the observed effect is related to altered TDP-43 function, and regardless has important implications for understanding FTLD-U and ALS pathogenesis. Notably, another group reported transgenic mice overexpressing wild-type TDP-43 under control of the Prp promoter at similar levels to those shown here, and these mice were normal without an observable phenotype through 12 months of age (27). Future studies involving inducible transgenes or other strategies will likely be needed to address these issues.

Protein aggregates and dysfunction of protein degradation pathways such as the ubiquitin proteasome system and autophagy are a hallmark of neurodegenerative disease (28). However, whether protein aggregates are themselves toxic, or instead play a protective role by helping to sequester smaller toxic protein species (such as soluble oligomers) continues to be a matter of intense investigation (29). Soluble oligomers of amyloid-β can induce synaptic dysfunction, and may play a role in the pathogenesis of Alzheimer's disease (30). Similarly, deleterious cellular effects including inhibition of the ubiquitin proteasome system leading to neurodegeneration can be seen with soluble disease mutant forms of α-synuclein, prion protein, and proteins with polyglutamine expansions (31–33). Our findings in the Prp-TDP43^{A315T} mice similarly indicate that selective neurotoxicity of the TDP43^{A315T} protein does not require the development of large cytoplasmic TDP-43 aggregates. Instead, these data suggest that soluble TDP43^{A315T} either directly or indirectly (via disrupting splicing/stability of certain mRNA species) alters protein degradation pathways, thereby promoting the accumulation of ubiquitinated proteins and neurodegeneration in selected neuronal populations.

Materials and Methods

Generation of Prp-TDP43^{A315T} Mice. A cDNA encoding human TDP-43 with an N-terminal Flag tag and the A315T mutation was generated by standard PCR mutagenesis using the full length human TDP-43 cDNA as a template. The Flag sequence was placed immediately after the start methionine, with the final sequence ''M-DYKDDDK-SEYIR…'' The resulting cDNA (Flag-TDP43^{A315T}) with the A315T mutation was sequenced confirmed, then blunt cloned into the *Xho*I site of the MoPrp.Xho plasmid (ATCC#JHU-2). The linearized construct was injected into eggs from hybrid C57Bl6/JxCBA mice. Eight founders were obtained. Of these, two died before weaning and were not able to be analyzed, five carried the transgene but did not express protein, with the remaining founder being the Prp-TDP43^{A315T} transgenic line. Mice were backcrossed to C57Bl6/J for two generations, with F1 and F2 mice used for pathologic and biochemical analysis. After developing a gait disorder the mice were monitored daily. Mice unable to right themselves for 15 s after being placed on their back were euthanized. Prp-TDP43<A315T> mice are available through The Jackson Laboratory Repository. They are assigned JAX Stock No. 010700.

Immunohistochemical Staining. Mice were perfused transcardially with 4% paraformaldehyde in 0.1 M phosphate buffer, pH 7.4 and paraffin-embedded. Four-micrometer-thick sections of brain and spinal cord were cut using a microtome and immunohistochemistry was carried out using the avidin-biotin complex detection technique (Vectastain ABC kit; Vector Laboratories). Sections were deparaffinized and rehydrated, endogenous peroxidases were quenched with 0.3% H_2O_2 in water for 30 min. Sections were next pretreated with citrate buffer and formic acid for 5 min to enhance immunoreactivity, developed using 3,3′-diaminobenzidine, and counterstained with hematoxylin after immunohistochemistry. Primary antibodies included anti-FLAG (1:500) (Sigma); rabbit polyclonal antibody recognizing amino acids 1–260 of TDP-43 (1:4000) (ProteinTech Group); rabbit polyclonal to the C-terminal amino acids 350–414 of TDP-43 (1:500) (Novus); anti-ubiquitin antibody MAb 1510 (1:500) (Chemicon); anti-GFAP rabbit polyclonal (1:500) (Dako); anti-synuclein (1:500) and PHF1 (1:500) (gifts from Paul Kotzbauer, Washington University); SMI-32 (Covance, 1:500); CD11b (Serotec, 1:500). Nissl staining and hematoxylin/eosin staining were performed using standard methods. For CD11b staining, mice were perfused as above, brains were cryoprotected in 30% sucrose, and 50-μm sections were performed on a sliding frozen microtome. Slides were visualized using either an Olympus BX-51 upright microscope, or using a Nanozoomer automated microscope (Hamamatsu). Double-labeling immunofluorescence was performed on fixed paraffin-embedded sections of brain and spinal cord using the same primary antibodies against ubiquitin MAb1510 (1:500), rabbit polyclonal N-terminal TDP-43 (1:500), and rabbit polyclonal C-terminal TDP-43 (1:500), using Alexa Fluor 488- and Cy3 or 594-conjugated secondary antibodies (Molecular Probes) followed by cover slipping with Vectashield-DAPI mounting medium (Vector Laboratories).

Muscle and Nerve Histology, Motor Neuron, and Axon Quantitation. Gastrocnemius and tibialis anterior muscles were dissected fresh, immediately frozen in isopentane cooled in liquid nitrogen, and cryostat sections of gastrocnemius and tibialis anterior muscles were cut onto slides and stained with hematoxylin and eosin. For plastic sections, lower thoracic spinal cords were embedded in epon and 1-μm-thick sections were cut, stained with toluidine blue and examined for

the features of axonal degeneration in the corticospinal tract and lateral columns. For spinal cord axon counts, 100× photomicrographs were taken in the region of the dorsal corticospinal tract or lateral columns from 1-μm-thick plastic sections from lower thoracic spinal cords from nontransgenic ($n = 3$) and Prp-TDP43^{A315T} ($n = 3$) mice. Intact and degenerated axons were counted using ImageJ software, and normalized to area. The pure motor and sensory branches of the femoral nerve were dissected from the mice, and toluidine blue stained 1-μm plastic sections were performed. Intact myelinated axons were counted from 20× images of the entire motor and sensory femoral nerve branches. For spinal motor neuron quantitation, mice were perfused ($n = 3$ of each genotype) with 4% paraformaldehyde, and the L3–L5 region of the spinal cord was removed and paraffin embedded. Serial 10-μm sections were performed, and with every 10th section placed on a slide (≈5 sections/slide). Sections were Nissl stained, and the entire slide imaged using the Nanozoomer automated microscope. The number of cells in the ventral horn with an area of greater than or equal to 600 μm^2 were counted, and then averaged from at least 15 nonadjacent sections from the L3–L5 region of each animal.

Electromyography. Animals were anesthetized with avertin, and placed in a prone position on a thermal pad at 37 °C for the examination. EMG recordings using a Viking Quest portable EMG machine (Nicolet) were obtained using a 27-gauge, Teflon-coated, monopolar needle electrode with a 70 × 500 μm recording surface (PRO-37SAF; Electrode Store). A 29-gauge reference needle electrode (GRD-SAF; Electrode Store) was inserted s.c. in close approximation to the recording electrode. A subdermal ground electrode was placed on the back. The recording electrode was inserted into the tibialis anterior (TA) or gastrocnemius/soleus muscles, and spontaneous electrical activity was recorded for 90 s.

Biochemistry and Immunoblotting. For soluble fractions of mouse cortex and lumbar spinal cord were extracted at 5 mL/g (wt/vol) with protein buffer (50 mM Tris, 150 mM NaCl, 1 mM EDTA, 1 mM DTT, 1% Triton X-100, and a mixture of protease and phosphatase inhibitors), sonicated, and centrifuged at either 20,000 × *g* at 4 °C, or 100,000 × *g* at 4 °C for 30 min. For serial fractionation samples were extracted at 5 mL/g (wt/vol) with low-salt buffer (10 mM Tris, pH 7.5, 5 mM EDTA, 1 mM DTT, 10% sucrose, and protease inhibitors), high-salt buffer (HS = low salt buffer, 1% Triton X-100, and 0.5 M NaCl), myelin flotation buffer (HS buffer + 30% sucrose), sarkosyl buffer (LS + 1% sarkosyl + 0.5 M NaCl), followed by urea buffer (7 M urea, 2 M thiourea, 4% CHAPS, 30 mM Tris, pH 8.5). Samples were analyzed by electropheresis and blotting, and membranes were probed with either anti-Flag antibody (Sigma) 1:1,000; or anti-TDP43 (amino acids 1–260) 1:1,000 (Proteintech).

ACKNOWLEDGMENTS. We thank David Holtzman, Chris Weihl, William Seeley, and Jeffrey Milbrandt for discussion and critical reading of the manuscript, and Nina Panchenko, and Sherry Clark for assistance with mouse husbandry. This work was supported by National Institutes of Health grant NS055980 (to R.H.B), the Neuroscience Blueprint Core Grant NS057105 (to Washington University), the Hope Center for Neurological Disorders, the McDonnell Center for Cellular and Molecular Neurobiology, Muscular Dystrophy Association Grant 135428, and the Children's Discovery Institute. R.H.B. holds a Career Award for Medical Scientists from the Burroughs Wellcome Fund.

1. Seeley WW (2008) Selective functional, regional, and neuronal vulnerability in frontotemporal dementia. *Curr Opin Neurol* 21:701–707.
2. Cleveland DW, Rothstein JD (2001) From Charcot to Lou Gehrig: Deciphering selective motor neuron death in ALS. *Nat Rev Neurosci* 2:806–819.
3. Pasinelli P, Brown RH (2006) Molecular biology of amyotrophic lateral sclerosis: Insights from genetics. *Nat Rev Neurosci* 7:710–723.
4. Murphy JM, et al. (2007) Continuum of frontal lobe impairment in amyotrophic lateral sclerosis. *Arch Neurol* 64:530–534.
5. Lomen-Hoerth C, Anderson T, Miller B (2002) The overlap of amyotrophic lateral sclerosis and frontotemporal dementia. *Neurology* 59:1077–1079.
6. Neumann M, et al. (2006) Ubiquitinated TDP-43 in frontotemporal lobar degeneration and amyotrophic lateral sclerosis. *Science* 314:130–133.
7. Buratti E, Baralle FE (2008) Multiple roles of TDP-43 in gene expression, splicing regulation, and human disease. *Front Biosci* 13:867–878.
8. Gitcho MA, et al. (2008) TDP-43 A315T mutation in familial motor neuron disease. *Ann Neurol* 63:535–538.
9. Kabashi E, et al. (2008) TARDBP mutations in individuals with sporadic and familial amyotrophic lateral sclerosis. *Nat Genet* 40:572–574.
10. Van Deerlin VM, et al. (2008) TARDBP mutations in amyotrophic lateral sclerosis with TDP-43 neuropathology: A genetic and histopathological analysis. *Lancet Neurol* 7:409–416.
11. Sreedharan J, et al. (2008) TDP-43 mutations in familial and sporadic amyotrophic lateral sclerosis. *Science* 319:1668–1672.
12. Yokoseki A, et al. (2008) TDP-43 mutation in familial amyotrophic lateral sclerosis. *Ann Neurol* 63:538–542.
13. Lagier-Tourenne C, Cleveland DW (2009) Rethinking ALS: The FUS about TDP-43. *Cell* 136:1001–1004.
14. Kwiatkowski TJ, Jr, et al. (2009) Mutations in the FUS/TLS gene on chromosome 16 cause familial amyotrophic lateral sclerosis. *Science* 323:1205–1208.
15. Vance C, et al. (2009) Mutations in FUS, an RNA processing protein, cause familial amyotrophic lateral sclerosis type 6. *Science* 323:1208–1211.
16. Borchelt DR, et al. (1996) A vector for expressing foreign genes in the brains and hearts of transgenic mice. *Genet Anal* 13:159–163.
17. Cairns NJ, et al. (2007) Neuropathologic diagnostic and nosologic criteria for frontotemporal lobar degeneration: Consensus of the Consortium for Frontotemporal Lobar Degeneration. *Acta Neuropathol* 114:5–22.
18. Leigh PN, et al. (1991) Ubiquitin-immunoreactive intraneuronal inclusions in amyotrophic lateral sclerosis. Morphology, distribution, and specificity. *Brain* 114:775–788.
19. Molnar Z, Cheung AF (2006) Towards the classification of subpopulations of layer V pyramidal projection neurons. *Neurosci Res* 55:105–115.
20. Davidson Y, et al. (2007) Ubiquitinated pathological lesions in frontotemporal lobar degeneration contain the TAR DNA-binding protein, TDP-43. *Acta Neuropathol* 113:521–533.
21. Charcot JM, Joffroy A (1869) Deux cas d'atrophie musculaire progressive avec les lesions de la substance grise et faiscaux anterolateraux de la moelle epiniere. *Archives de Physiologic Normale et Pathologique* 2:354–367, 629–649, 744–760.
22. Baloh RH, Rakowicz W, Gardner R, Pestronk A (2007) Frequent atrophic groups with mixed-type myofibers is distinctive to motor neuron syndromes. *Muscle Nerve* 36:107–110.
23. Zhang YJ, et al. (2007) Progranulin mediates caspase-dependent cleavage of TAR DNA binding protein-43. *J Neurosci* 27:10530–10534.
24. Igaz LM, et al. (2009) Expression Of TDP-43 C-terminal fragments in vitro recapitulates pathological features of TDP-43 proteinopathies. *J Biol Chem.*
25. Zhang YJ, et al. (2009) Aberrant cleavage of TDP-43 enhances aggregation and cellular toxicity. *Proc Natl Acad Sci USA* 106:7607–7612.
26. Ayala YM, Misteli T, Baralle FE (2008) TDP-43 regulates retinoblastoma protein phosphorylation through the repression of cyclin-dependent kinase 6 expression. *Proc Natl Acad Sci USA* 105):3785–3789.
27. Xu Y, et al. (2008) Generation and characterization of human TDP-43 transgenic mice. *Society for Neuroscience Abstracts, Annual Meeting Publications.*
28. Winklhofer KF, Tatzelt J, Haass C (2008) The two faces of protein misfolding: Gain- and loss-of-function in neurodegenerative diseases. *EMBO J* 27:336–349.
29. Haass C, Selkoe DJ (2007) Soluble protein oligomers in neurodegeneration: Lessons from the Alzheimer's amyloid beta-peptide. *Nat Rev* Mol Cell Biol 8:101–112.
30. Walsh DM, et al. (2002) Naturally secreted oligomers of amyloid beta protein potently inhibit hippocampal long-term potentiation in vivo. *Nature* 416:535–539.
31. Klement IA, et al. (1998) Ataxin-1 nuclear localization and aggregation: Role in polyglutamine-induced disease in SCA1 transgenic mice. *Cell* 95:41–53.
32. Stefanis L, Larsen KE, Rideout HJ, Sulzer D, Greene LA (2001) Expression of A53T mutant but not wild-type alpha-synuclein in PC12 cells induces alterations of the ubiquitin-dependent degradation system, loss of dopamine release, and autophagic cell death. *J Neurosci* 21:9549–9560.
33. Kristiansen M, et al. (2007) Disease-associated prion protein oligomers inhibit the 26S proteasome. *Mol Cell* 26:175–188.